

# Multi-Doppler Compensation in Wireless Communication Systems

Raghav Gupta  
Electrical Engineering  
IIT Bombay, India  
Email: raghavgupta0110@gmail.com

**Abstract**—In the present scenario, the technique employed to tackle the doppler present in the received signal is to find the dominant Doppler frequency in the received signal for all path and compensate for the same. but the drawback with this is that in wireless environment, each path may have more than one Doppler and all path will have different Dopplers. So, in this paper our aim is to concentrate on the multiple Doppler present on the single path environment. The signal consist of two or more Doppler in it and, so constituting a need to compensate for each Doppler to get a better estimate of the transmitted signal.

## I. INTRODUCTION

Spread spectrum is a widely employed data communication technique, and is the principle behind multiple access schemes using CDMA. Good diversity performance in multipath channels, jamming margin, low detectability, better frequency reuse in cellular services etc are some of the key advantages of CDMA. Notice that CDMA typically employs a wideband width, typically larger than the coherence bandwidth in wireless deployments. This leads to frequency selectivity and multipath effects, usually quantified in terms of the Delay spread. The channel here can be well modeled by a tapped delay line model [1]. In the presence of a reasonable number of multipaths, CDMA receivers have good diversity performance [1].

Synchronization of the transmitter and receiver is a major bottleneck in achieving optimal performance in a wireless communication system. In addition to clock offsets, Doppler spread is another reason for carrier frequency fluctuations in wireless systems. Usual Doppler compensation models assume a single dominant Doppler frequency [1]–[3], whereas the performance can improve when multiple Doppler frequencies are accounted for.

One of the algorithm used for Doppler frequency correction deals with frequency search [4]. In this technique the data is correlated with the preamble being shifted by frequency  $f_i$ , the frequency being changed to cover a certain range in which the Doppler frequency lies. The frequency having the maximum correlation is taken as the CFO for that received signal as given by [5]. Another technique used for CFO estimation is given by [6]. This technique uses the spectrum of the received signal and corrects the CFO by calculating the shift in the spectrum from the dc level. [7] and [8] uses the FFT based frequency offset estimation to correct CFO. All these techniques deals with estimation of a single dominant Doppler frequency and correcting it.

In this paper we consider multi-Doppler compensation. We first consider narrowband wireless channels where the transmitted signals reach the receiver through different propagation paths with comparable delays. Algorithms to identify the multiple Doppler frequencies are proposed, along with further tracking of the variations. We then extend this to wideband systems using spread spectrum. In the latter case, multi-paths may have different Doppler spreads as well as time delays due to Delay spread.

The organization of the paper is as follows. Section II details the system models for both narrowband and wideband communication systems. Doppler correction algorithms for the narrowband models are given in Section III, whereas their wideband counterparts are considered in Section IV. Finally, Section V concludes the paper.

## II. SYSTEM MODEL

Keeping spread-spectrum in mind, let us consider a data signal  $d_i$  which is composed of  $\pm 1$ s. The transmitted baseband signal is given by

$$x(t) = \sum_{n \in \mathbb{Z}} d_n c(t - nT), \quad (1)$$

where  $T$  is the bit duration,  $d_n$  is the user data signal,  $n$  is the bit index and  $c$  is the spreading signal given by

$$c(t) = \sum_{k=0}^{K-1} m_k g(t - kT_c). \quad (2)$$

Here  $T_c$  is the chip duration,  $m_k$  is the code sequence of spreading factor  $K$ ,  $g(t)$  is a rectangular pulse in  $[0, T_c)$ , and  $T = KT_c$ .

The transmitted signal  $x(t)$  is passed through the wireless channel with  $L$  taps. At the receiver, we get

$$y(t) = \sum_{i=0}^{L-1} x(t - \tau_i) \alpha_i e^{-j2\pi f_c \tau_i} e^{-j2\pi f_{di} t} + z(t). \quad (3)$$

Here  $f_{di}$  is the Doppler frequency in the  $i^{th}$  multipath component,  $\alpha_i$  is the gain of the  $i^{th}$  path and  $z(t)$  represents white Gaussian noise.

### A. Narrowband System model

For a narrowband system, we will assume that the transmitted signal is same for all the path, i.e. the delay  $\tau_i$  can be neglected [9].

$$x(t) \approx x(t - \tau_i) \quad (4)$$

So, taking the above mentioned narrowband assumption into account, the equation 3 changes to

$$y(t) \approx x(t) \left( \sum_{i=0}^k \alpha_i e^{-j2\pi f_{di}t} \right) + z(t) \quad (5)$$

So, in a narrowband scenario, all the paths reach at the same time with different carrier frequency offset or Doppler.

### B. Wideband System Model

Equation 3 represents the wideband system model used for tracking the multiple Doppler phenomenon and for correcting the same, i.e.,

$$y(t) = \sum_{i=0}^k x(t - \tau_i) \alpha_i e^{-j2\pi f_c \tau_i} e^{-j2\pi f_{di}t} + z(t)$$

## III. ALGORITHMS FOR NARROWBAND MODELS

We assume that time-synchronization is already done, and focus only on frequency estimation. The algorithms also need the assumption that coherence time is not too small, that the Doppler frequencies are nearly constant during each estimation stage, but can vary across stages.

### A. Narrowband System

Our first objective is to find the Doppler frequencies present in the signal given by equation 5. First, we square  $y(t)$  to get the following signal:

$$y_{sq}(t) = |y(t)|^2 \quad (6)$$

$$y_{sq}(t) = x^2(t) \left| \sum_{i=0}^k \alpha_i e^{-j2\pi f_{di}t} \right|^2 + z_{\text{eff}}(t), \quad (7)$$

Where  $z_{\text{eff}}(t)$  is the effective noise given by

$$z_{\text{eff}}(t) = 2x(t) \left( \sum_{i=0}^k \alpha_i e^{-j2\pi f_{di}t} \right) z(t) + |z(t)|^2$$

Since  $x(t)$  signal is composed of  $\pm 1$  so squaring gets rid of that term from equation 7, thereby reducing the equation to:

$$y_{sq}(t) = \left| \sum_{i=0}^k \alpha_i e^{-j2\pi f_{di}t} \right|^2 + z_{\text{eff}}(t) \quad (8)$$

Other than the noise term, the dominant frequency components of  $y_{sq}(t)$  are

$$2f_{di}, \quad i = 1 \text{ to } k \quad \text{and} \quad (9)$$

$$f_{di} + f_{dj}, \quad i = 1 \text{ to } k, \quad j = 1 \text{ to } k, \quad i \neq j. \quad (10)$$

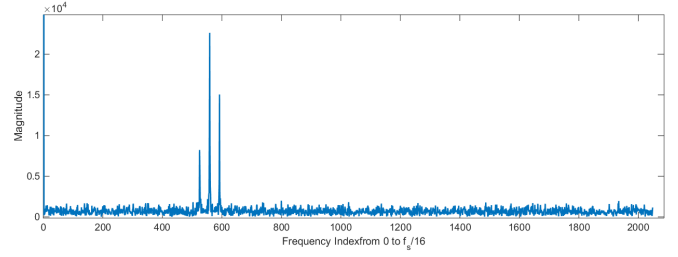


Fig. 1. FFT plot depicting the Doppler frequencies (A small section of the FFT plot has been shown to highlight the presence of the Doppler frequencies)

Thus, the Fourier Transform of  $y_{sq}(t)$  will reveal the dominant frequency components. This is illustrated in the figure below.

The next task is to identify the actual Doppler frequencies from the identified frequency components, based on (9). We will illustrate this for 6 dominant peaks in the DFT plot of the samples from  $y_{sq}(t)$ . Assume that all Doppler components are positive. Notice that 6 peaks correspond to 3 Doppler frequencies. The maximal frequency component can be seen to be twice the maximal Doppler frequency. Similarly the minimal frequency component is twice the minimal Doppler frequency. Thus, the highest Doppler frequency  $f_{d1}$  and least component  $f_{d3}$  can be identified.

Now out of the remaining frequencies present after removing  $f_{d1}$  and  $f_{d3}$ , the maximum frequency component present is  $f_{d2} + f_{d3}$ . So, Let

$$f_{sum} = f_{d2} + f_{d3}. \quad (11)$$

So subtracting  $f_{d3}$  from  $f_{sum}$ , we will get  $f_{d2}$  as

$$f_{d2} = f_{sum} - f_{d3}. \quad (12)$$

The technique can be used for measurement of up to 4 Doppler frequencies. The FFT plot of the squared signal  $y_{sq}(t)$  is shown in figure 1. Two Doppler frequencies are present in the signal. Thus, the FFT plot has three peaks as per the equation 9.

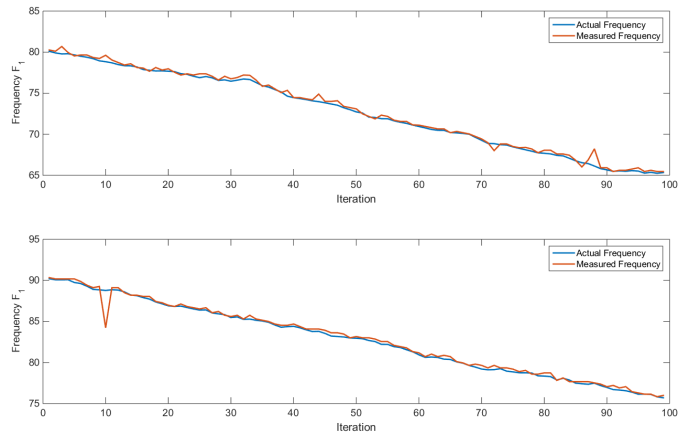


Fig. 2. Doppler Frequency measurement

Figure 2 shows the actual frequency values vs the measured values calculated at an interval of  $F_l$ .

## B. Tracking Doppler Components

The above-mentioned algorithm is primarily used as an initial estimate of the Doppler components. One can repeat this estimation in periodic intervals or when the available synchronization is lost. Once the initial synchronization is acquired, it is more efficient to track the variation in Doppler frequencies. We track the intermediate frequencies using a Kalman filter.

In between two  $F_l$  periods, the frequency change is given by the following equation:

$$f(n) = \beta f(n-1) + (1-\beta)w(n) \quad (13)$$

where,  $w$  represents zero mean unit variance Gaussian noise. The value  $\beta$  is near one for slow variations in time.

The Kalman filter algorithm used for estimating the present state involves two steps given in algorithm III-B.

- 1: **Prediction:** In this step, the present estimate of the state vector is estimated only from the knowledge of the previous estimate. Following equations govern this step.

$$X_k^- = A_{k-1}X_{k-1} + B_kU_k \quad (14)$$

$$P_k^- = A_{k-1}P_{k-1}A_{k-1}^T + Q_{k-1} \quad (15)$$

where  $X_k^-$  and  $P_k^-$  respectively represent the predicted present state  $X_k$  and the covariance of the state  $P_k$ , before acquiring the measurement  $Y_k$ .

- 2: **Update:** In this step, the current state of the system is estimated given the measurement in that step. Following equations govern this step.

$$V_k = Y_k - H_kX_k^- \quad (16)$$

$$S_k = H_kP_k^-H_k^T + R_k \quad (17)$$

$$K_k = P_k^-H_kS_k^{-1} \quad (18)$$

$$X_k = X_k^- + K_kV_k \quad (19)$$

$$P_k = P_k^- - K_kS_kK_k^T \quad (20)$$

where  $X_k$  and  $P_k$  are the estimated present state and covariance of the state after seeing the measurement.  $Y_k$  is the measurement.  $V_k$  is the innovation.  $S_k$  is the measurement prediction covariance.  $K_k$  is filter gain which gives correction to be made on prediction.  $H_k$  is the measurement matrix.

Using Kalman filter, we need to track the variations in the Doppler frequencies. The state variables take following values in the frequency tracking algorithm, with some modifications.

- The matrix  $H$  is an identity matrix
- $B$  is a zero matrix. assuming that initial state is zero.
- when  $k \% F_l == 0$ 
  - $A_k = A$
  - $Q_k = Q$
  - $d = X_{meas} - X_k^-$

- $V = d$  when  $|d| < \epsilon$
- $V = \text{zero vector}$  otherwise

$Q$  is the covariance matrix of noise  $w$  given in equation 13.  $R$  is covariance matrix of the noise in equation 5.  $K$  is the Kalman gain.  $X$  is the state of the frequency which we want to track.  $X_{meas}$  is the measured Doppler frequency. As, it is known that the frequency will not vary much in one step so, only if the measured frequency is within range of  $\epsilon$  from previous estimated value the measurement is considered to be accurate. Otherwise we consider the innovation to be zero.

The figure 3 shows the frequency tracking plot using the Kalman filter for two Doppler frequencies.

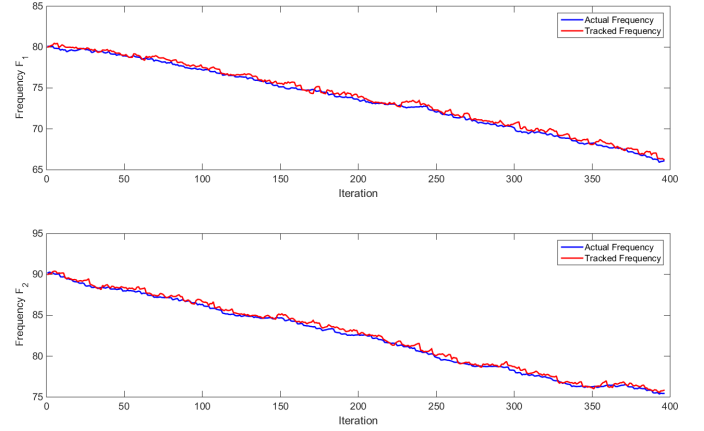


Fig. 3. Doppler Frequency tracking using Kalman filter

The transmitted signal is BPSK in narrowband scenario. After finding the Doppler frequencies, we need to decode the received signal to get the transmitted bits. For that, first of all we need to find the starting sample in the frame. A frame consists of preamble/pilot using which one can localize the frame position in the given data stream. So, correlating the data stream with the pilot/preamble will give the peak at the sample where the preamble starts, thereby giving the location of the start of the frame. Also it provides the amplitude for weighing that bit during weighted average at last. Directly correlating it with the data sequence would not give results since the data is having Doppler shift. So, instead we correlate the data stream with preamble which is also Doppler shifted, the Doppler shift is being estimated by algorithm III-B. After decoding the data with all the Doppler frequencies, we do weighted average of the decoded signals with weights being taken from the fraction of the amplitude of correlation peak.

## IV. ALGORITHMS FOR WIDEBAND MODELS

Doppler frequency estimation and correction in wideband CDMA system is same as that in narrowband systems. The algorithms devised for the Doppler frequencies correction of narrowband signal works for wideband system with some modification. In Wideband CDMA scenario, the procedure for decoding the bits after finding the Doppler frequency changes. The decoding is done by correlating with the CDMA code present in the received signal.

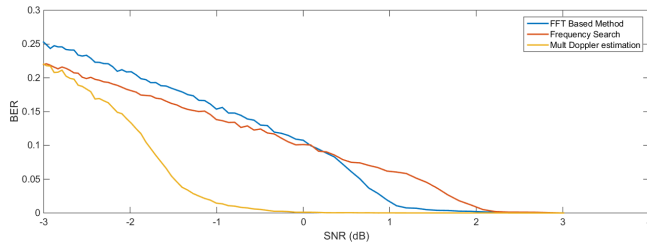


Fig. 4. BER vs SNR

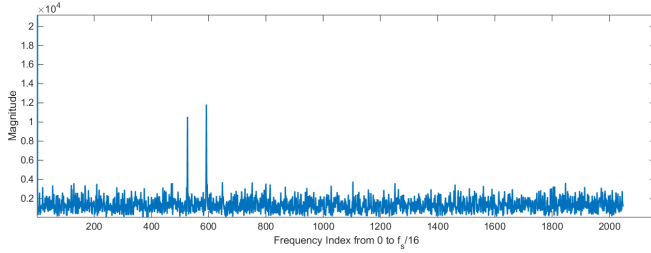


Fig. 5. FFT plot depicting the Doppler frequencies

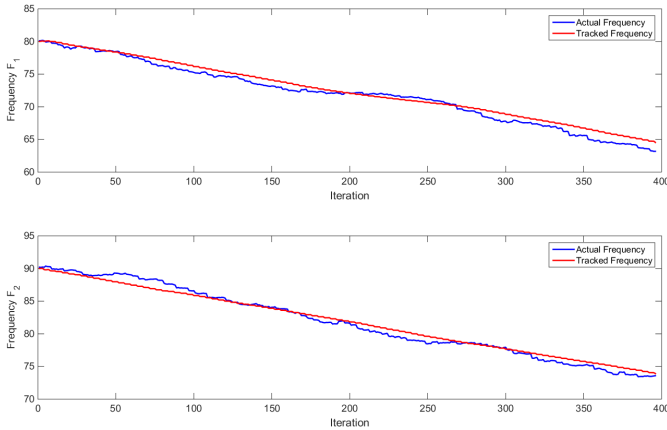


Fig. 6. Doppler Frequency tracking using Kalman filter for wideband (CDMA) signal

So in case of a wideband CDMA signal modulated with BPSK modulation scheme, the algorithm used for estimating and tracking the multiple Doppler frequency i.e., algorithm III-B remains the same as these algorithm had only requirement of transmitted signal being BPSK modulated.

In measurement of Doppler frequencies, as can be seen from figure 5 only the Doppler frequency components are present in the spectrum with frequency being doubled. i.e.,

$$2f_{di}, i = 1 \text{ to } k \quad (21)$$

So one needs to find just the peaks, divide them by two to get the Doppler frequencies.

The FFT plot of the squared signal  $y_{sq}(t)$  is shown in figure 5 for a wideband signal with two multipath. The figure 6 shows the Doppler frequency tracking plot using algorithm III-B for wideband (CDMA) system. BER plot for

the wideband system using CDMA with code size of 127 is compared with the frequency search method and the FFT based method as show in figure 7.

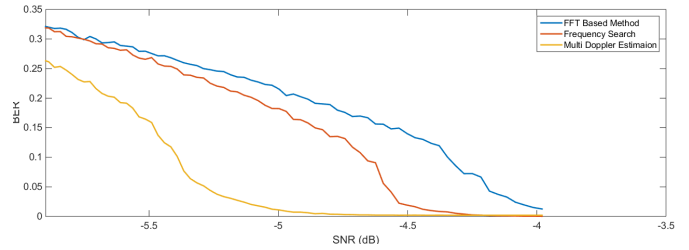


Fig. 7. BER vs SNR

## V. CONCLUSION

The overall process of frequency estimation, tracking and correction is given as a flow graph in Figure 8. The flow graph consists of four parts namely, frequency measurement, frequency tracking, frequency Correction and signal decoding. We have shown than multi-Doppler estimation can provide significant advantages over standard approaches correcting a single frequency.



Fig. 8. Flow graph for multiple Doppler frequency correction

## REFERENCES

- [1] J. G. Proakis and M. Salehi, *Digital Communications*. McGraw Hill International, 2008.
- [2] A. A. Nasir, S. Durrani, H. Mehrpouyan, S. D. Blostein, and R. A. Kennedy, "Timing and carrier synchronization in wireless communication systems: a survey and classification of research in the last 5 years," *EURASIP Journal on Wireless Communications and Networking*, vol. 2016, no. 1, p. 180, 2016.
- [3] D. Zhao, L. Xi, X. Tang, W. Zhang, Y. Qiao, and X. Zhang, "Digital pilot aided carrier frequency offset estimation for coherent optical transmission systems," *Optics express*, vol. 23, no. 19, pp. 24822–24832, 2015.
- [4] L. Dai, Z. Wang, J. Wang, and J. Song, "Joint code acquisition and doppler frequency shift estimation for gps signals," in *2010 IEEE 72nd Vehicular Technology Conference - Fall*, pp. 1–5, Sept 2010.
- [5] M. Wax, "The joint estimation of differential delay, doppler, and phase (corresp.)," *IEEE Transactions on Information Theory*, vol. 28, no. 5, pp. 817–820, 1982.
- [6] F. Harris, E. Venosa, X. Chen, and C. Dick, "Band edge filters perform non data-aided carrier and timing synchronization of software defined radio qam receivers," in *Wireless Personal Multimedia Communications (WPMC), 2012 15th International Symposium on*, pp. 271–275, IEEE, 2012.
- [7] Y. Cao, S. Yu, J. Shen, W. Gu, and Y. Ji, "Frequency estimation for optical coherent mpsk system without removing modulated data phase," *IEEE Photonics Technology Letters*, vol. 22, no. 10, pp. 691–693, 2010.
- [8] Y. Liu, Y. Peng, S. Wang, and Z. Chen, "Improved fft-based frequency offset estimation algorithm for coherent optical systems," *IEEE Photon. Technol. Lett.*, vol. 26, no. 6, pp. 613–616, 2014.
- [9] A. Goldsmith, "Lecture 4 - ee359: Wireless communications - autumn 2017 statistical fading models & narrowband models." [https://web.stanford.edu/class/ee359/pdfs/lecture4\\_handout.pdf](https://web.stanford.edu/class/ee359/pdfs/lecture4_handout.pdf), 2017.